Dephasing of ultracold cesium $80D_{5/2}$-Rydberg Electromagnetically Induced Transparency

Yuechun Jiao,[1,3] Liping Hao,[1] Jingxu Bai,[1] Jiabei Fan,[1] Zhengyang Bai,[2,3*] Weibin Li,[4] Jianming Zhao,[1,3,5] Suotang Jia,[1,3]

[1] *State Key Laboratory of Quantum Optics and Quantum Optics Devices, Institute of Laser Spectroscopy, Shanxi University, Taiyuan 030006, P. R. China*
[2] *State Key Laboratory of Precision Spectroscopy, East China Normal University, Shanghai 200062, People's Republic of China*
[3] *Collaborative Innovation Center of Extreme Optics, Shanxi University, Taiyuan 030006, China*
[4] *School of Physics and Astronomy and Centre for the Mathematics and Theoretical Physics of Quantum Non-equilibrium Systems, University of Nottingham, Nottingham NG7 2RD, United Kingdom*
[*] *zhybai@lps.ecnu.edu.cn*
[5] *zhaojm@sxu.edu.cn*

Abstract: We study Rydberg electromagnetically induced transparency (EIT) of a cascade three-level atom involving $80D_{5/2}$ state in a strong interaction regime employing a cesium ultracold cloud. In our experiment, a strong coupling laser couples $6P_{3/2}$ to $80D_{5/2}$ transition, while a weak probe, driving $6S_{1/2}$ to $6P_{3/2}$ transition, probes the coupling induced EIT signal. At the two-photon resonance, we observe that the EIT transmission decreases slowly with time, which is a signature of interaction induced metastability. The dephasing rate γ_{OD} is extracted with optical depth $\mathrm{OD} = \gamma_{\mathrm{OD}} t$. We find that the optical depth linearly increases with time at onset for a fixed probe incident photon number R_{in} before saturation. The dephasing rate shows a nonlinear dependence on R_{in}. The dephasing mechanism is mainly attributed to the strong dipole-dipole interactions, which leads to state transfer from $nD_{5/2}$ to other Rydberg states. We demonstrate that the typical transfer time $\tau_{0(80D)}$ obtained by the state selective field ionization technique is comparable with the decay time of EIT transmission $\tau_{0(\mathrm{EIT})}$. The presented experiment provides a useful tool for investigating the strong nonlinear optical effects and metastable state in Rydberg many-body systems.

1. Introduction

Due to the strong interaction ($\propto n^{11}$ with n principal quantum number) [1], Rydberg atoms provides an ideal platform to implement quantum information and quantum simulation [2–5] and investigate interaction induced cooperative optical nonlinearities [6]. The optical nonlinear effects are induced by Rydberg atom interactions [7, 8], i.e., van der Waals (vdW) interactions [9–11] and dipole-dipole interactions [12, 13]. Strong atomic interactions can be effectively mapped onto photon-photon interactions via electromagnetically induced transparency (EIT) [6]. Due to the cooperative effects, the optical nonlinearity can be greatly enhanced [6, 14–16]. Based on this, Rydberg EIT experiments are employed to measure a radio-frequency electric field [17] with a room-temperature cell, and to realize few-photon optical nonlinearities [18–21] with an ultracold sample, such as the efficient single photon generation [18], entanglement generation between light and atomic excitations [20], single-photon switches [16, 19, 22] and transistors [21, 23, 24]. The resonant dipole-dipole interaction between two individual Rydberg atoms [25] is angular dependent. Recently, the anisotropic Rydberg interaction have been adopted to investigate Rydberg polaritons by using Rydberg nD-state [26].

In this work, we present a Rydberg EIT spectrum of a cascade three-level cesium atom

involving $80D_{5/2}$ state in a dipole trap. Under the two-photon resonance condition, we observe that EIT transmission displays a slow decrease with time. This could be a signature of interaction induced metastability [27,28]. Due to the large dipole matrix elements, the cesium nD-state atom has strong dipole interactions with energetically close $(n+1)P$ state. We find that, strong dipole interactions between the nD and $(n+1)P$ state leads to a fast decay of nD to $(n+1)P$ state, and the dephasing of the transmission spectrum. A theoretical model is built to understand EIT dephasing mechanism. The nonlinear dependence on dephasing rate has also been investigated.

The remainder of the article is arranged as follows. In Sec. 2, we introduce our experimental setup. In Sec. 3, we reveal Rydberg EIT spectrum and its dephasing experimentally. In Sec. 4, we present a simple theoretical model to reveal EIT dephasing mechanism. In Sec. 5, we measure the fast decay process on $80D_{5/2}$ state. Finally, we summarize the main results obtained in this work.

2. Experimental Setup

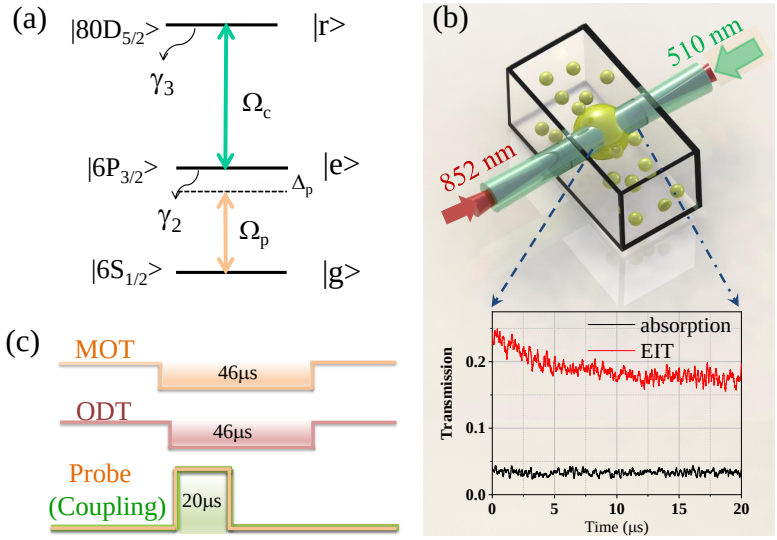

Fig. 1. (a) Atomic level scheme. A weak probe laser field with Rabi frequency Ω_p drives the lower transition, $|g\rangle = |6S_{1/2}, F = 4\rangle \rightarrow |e\rangle = |6P_{3/2}, F' = 5\rangle$. The strong coupling laser (Rabi frequency Ω_c) couples the transition $|e\rangle \rightarrow |r\rangle = |80D_{5/2}\rangle$. (b) Experiment setup. The coupling and probe beams are counter-propagated through the MOT center and overlap with the dipole trap beam. The transmission of probe beam is detected with a single photon counting module (SPCM). The inset shows EIT dephasing behaviors (red) and probe absorption (black; without coupling beam). The data are taken by the sum of 3000 experimental cycles. (c) Experimental timing. After switching off the MOT and dipole trap beams, Rydberg-EIT coupling and probe lasers are turned on for 20 μs, during which the probe laser frequency is ramped through the $|g\rangle \rightarrow |e\rangle$ transition over ±15 MHz by a double-passed AOM.

Our experiment is performed in a cesium magneto-optical trap (MOT) with optical dipole trap (ODT). The beam waist of dipole trap is 45 μm. A schematic of relevant levels and the experimental setting are shown in Fig. 1 (a) and (b). A three-level system, shown in Fig. 1(a), consists of a ground state $|6S_{1/2}, F = 4\rangle$ ($|g\rangle$), intermediate state $|6P_{3/2}, F' = 5\rangle$ ($|e\rangle$) and

Rydberg state $|80D_{5/2}\rangle$ ($|r\rangle$). A weak probe beam (Rabi frequency Ω_p, 852-nm laser with a 100-kHz linewidth), provided by an external cavity diode laser (Toptica, DLpro), drives a lower transition and the frequency is stabilized to the $|6S_{1/2}, F = 4\rangle \rightarrow |6P_{3/2}, F' = 5\rangle$ transition using the polarization spectroscopy method. The coupling beam (Rabi frequency Ω_c) provided by a commercial laser (Toptica, TA-SHG110) with linewidth 1 MHz drives Rydberg transition, $|6P_{3/2}, F' = 5\rangle \rightarrow |80D_{5/2}\rangle$. The coupling laser frequency is stabilized to the Rydberg transition using a Rydberg EIT reference signal obtained from a cesium room-temperature vapor cell [29]. The weak probe laser and strong coupling laser, with respective Gaussian radius of 9 μm and 30 μm, are overlapped and counter-propagated through the MOT center, see Fig. 1(b). The probe laser is scanned using a double-passed acousto-optic modulator (AOM) that covers the lower transition. The transmission of the probe laser, Rydberg EIT spectrum, is detected with a single photon counting module (SPCM) and processed with *Labview* program. The glass MOT is surrounded by three pairs of field-compensation Helmholtz coils, which allow us to reduce stray magnetic fields via EIT Zeeman splitting, corresponding stray field less than 5 mG. In our experiment, the peak density of atomic cloud about 10^{11} cm^{-3} is measured by shadow imaging and the temperature of atomic cloud is about 100 μK. The estimated Rydberg density is 2.4×10^8 cm^{-3}.

The experimental timing is shown in Fig. 1(c) with the whole time 200 ms, corresponding to a repetition rate of 5 Hz. In each cycle, after turning off the trap beams, we switch on the coupling and probe lasers for 20 μs, during which the probe-laser frequency is swept across the $|6S_{1/2}, F = 4\rangle \rightarrow |6P_{3/2}, F' = 5\rangle$ transition to observe the EIT spectra in Fig.2 (a) or fixed on resonance to investigate the dephasing in Fig. 1(b) and Fig. 2(b), meanwhile the power is fixed using a proportional-integral-derivative controller (PID) feedback loop that controls the radio-frequency power supplied to the 852-nm AOM. The data shown in Fig. 1(b) is taken by the sum of 3000 cycles.

3. Experimental observation of Rydberg EIT and transmission dephasing

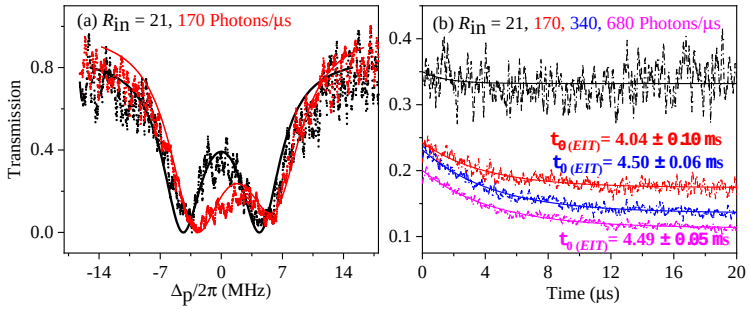

Fig. 2. (a) Rydberg-EIT spectra with a coupling laser, $\Omega_c/2\pi$ =10.6 MHz, resonant with the $|6P_{3/2}, F' = 5\rangle \rightarrow |80D_{5/2}\rangle$ transition, and a probe frequency scanning across the lower transition, $|6S_{1/2}, F = 4\rangle \rightarrow |6P_{3/2}, F' = 5\rangle$, at a probe-photon rate R_{in} = 21 photons/μs and 170 photons/μs, respectively. The solid lines are the fittings using the density matrix equation of a three-level atom. The EIT transmission displays a strong suppression and blue shift with increasing probe R_{in}. (b) EIT transmissions for the indicated probe photon input rates at two-photon resonance condition. The transmission remains same for R_{in} = 21 photons/μs, whereas decrease with R_{in} at the beginning and then decay with the EIT maintain time for larger R_{in} cases. The solid lines denote the exponential fittings. For higher R_{in} the characteristic time are $\tau_{0(EIT)}$ = 4.04 ± 0.10 μs, 4.50 ± 0.06 μs and 4.49 ± 0.05 μs, respectively.

Due to the quantum interference effect [30], the probe transmission T increases when the coupling and probe laser frequencies satisfy the two-photon resonance [see Fig. 1(a)]. Using the rotating wave approximation and in the interaction picture [31], the eigenstate of three-level Hamiltonian can be obtained with $|D\rangle \propto \Omega_c^*|g\rangle - \Omega_p|r\rangle$ at two-photon resonance. For conventional EIT, the system works in dark state and the probe pulse suffers little optical absorption. For the three-level scheme, all atoms are initially prepared in state $|g\rangle$. The EIT system can evolve to the dark state $|D\rangle$ with time $1/\gamma_2$. However, as shown in Fig. 1(b), in $nD_{5/2}$-Rydberg EIT system, the EIT transmission slowly decreases with time. Interesting, the time scale of the dephasing is much longer than the lifetime of intermediate state $|e\rangle$. The dipolar interaction can lead to many-body dephasing [26, 32] in case of Rydberg nD state.

We present EIT spectra with $80D_{5/2}$ Rydberg state in Fig. 2(a). The probe field is adopted as incident photon rates $R_{\rm in}$ = 21 photons/μs (black dashed line) and 170 photons/μs (red dashed line) with $\Omega_c = 2\pi \times 10.6$ MHz. It is found that the transmission decreases with increasing $R_{\rm in}$ and accompanies with the EIT-peak shift. The EIT transmission rate is around 40% for $R_{\rm in}$ = 21 photons/μs, and decreases to 20% when $R_{\rm in}$ increases to 170 photons/μs. We attribute the reduction of optical transmission to atomic interactions between Rydberg states. Besides, when $R_{\rm in}$ = 170 photons/μs, the EIT peak has a blue shift about 2.5 MHz compared with the case for $R_{\rm in}$ = 21 photons/μs. For Rydberg EIT, dark-state polariton is very sensitive to other Rydberg excitation in the strong interaction regime. This is because when two Rydberg polaritons propagate inside the medium with a distance r, they experience an interaction induced energy shift $U(r)$. It gives rise to a non-vanishing Im(χ) of probe beam where χ optical susceptibility of system and therefore leads to strong absorption and a shift on EIT spectra [6, 14, 15].

To further investigate the dephasing feature for nD state, we vary the probe-photon rate $R_{\rm in}$ with fixed coupling field $\Omega_c/2\pi$ =10.6 MHz. Both the coupling and probe lasers frequencies are on resonance. As shown in Fig. 2(b), the time dependence of the transmission is plotted with different $R_{\rm in}$. For low probe photon rates (i.e., $R_{\rm in}$ = 21 photons/μs), the transmission is almost a constant, but when increasing $R_{\rm in}$, transmission exhibits a slow decrease with time t. By fitting the data in panel (b) with the exponential function $T = A\exp(-t/\tau_{0(\rm EIT)}) + T_0$, the decay time $\tau_{0(\rm EIT)}$ = 4.04 ± 0.10 μs, 4.50 ± 0.06 μs and 4.49 ± 0.05 μs can be extracted for different $R_{\rm in}$. The decay time is much longer than the lifetime in state $|e\rangle$ (i.e., $1/\gamma_2 \sim 0.03\mu$s).

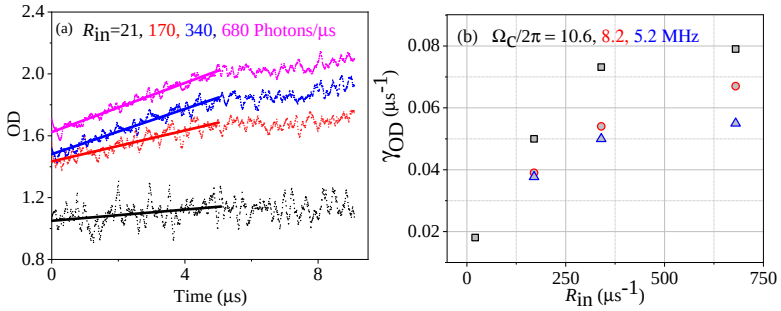

Fig. 3. (a) The optical depth of the $80D_{5/2}$ EIT transmission taken the logarithm of spectra in Fig. 2(b) for indicated photon incidence rates $R_{\rm in}$ at fixed $\Omega_c = 2\pi\times10.6$ MHz. The solid lines are linear fittings before t = 5 μs to the data to extract the dephasing rates $\gamma_{\rm OD}$. (b) The dephasing rates $\gamma_{\rm OD}$ as a function of $R_{\rm in}$ for coupling Rabi frequency $\Omega_c/2\pi$ = 10.6, 8.2 and 5.2 MHz, respectively.

In order to reveal the dephasing mechanism, we define the effective optical depth (OD) of the medium as the logarithm of transmission [i.e., OD = -ln(T)] [26]. The time evolution of OD is shown in Fig. 3(a) [corresponding to the results in Fig. 2(b)]. One sees that OD approximately

linearly increases with time before t = 5 μs. By neglecting saturation effects, we can redefine $OD = \gamma_{\rm OD} t$ where $\gamma_{\rm OD}$ reflects creation rate of optical density by decoupled impurities [26]. At small probe photons (i.e., $R_{\rm in} \lesssim 340\ \mu{\rm s}^{-1}$), the extracted rate $\gamma_{\rm OD}$ displays a linear increase with $R_{\rm in}$ and then saturates for large $R_{\rm in}$ [see Fig. 3(b)]. This is because the system is not fully in a blockade regime at small probe photons. Therefore, with increasing photon number, more Rydberg atoms are excited, which increase the dipole-dipole interaction, leading to increased $\gamma_{\rm OD}$. However, after the system enter fully blockade regime, we can't excite more Rydberg atoms so that the dephasing rate $\gamma_{\rm OD}$ shows saturation. This is a signature of many-body dephasing. We calculate the group velocity of probe photon is around 3920 m/s under our experiment condition with Ω_c = 10.6 MHz. By considering the length of our atomic cloud 1 mm, the propagation time of photon through the cloud is around 0.26 μs. The Rydberg blockade radius is about 10 μm for $80D_{5/2}$. Under this condition, almost 100 atoms can be excited to Rydberg state. Thus we can calculate that in one microsecond, the maximum number of Rydberg excitation is around 385, where $100\,{\rm atom}/0.26\,\mu{\rm s} \simeq 385\ /\mu{\rm s}$. Thus, the critical value for $R_{\rm in}$ is around 385 /μs. When the photon incidence rates $R_{\rm in}$ is smaller than 385 /μs, the system is not in the blockade regime. When increasing the intensity of the probe laser, the system can works in the full blockade regime. This estimation is agreed with the dephasing rates $\gamma_{\rm OD}$ in Fig. 3(b). We also change Ω_c and measure EIT dephasing rates $\gamma_{\rm OD}$ versus $R_{\rm in}$. The results show a similar nonlinear dependence on $R_{\rm in}$ [see Fig. 3(b)].

4. Analysis of EIT dephasing mechanism

The vdW interaction between $nD_{5/2}$ pair leads to energy level shifts and dipole interaction of $nD_{5/2}$ and nearest Rydberg states yield state transfer of $nD_{5/2}$ to other Rydberg states. We have found [33] that nD-$(n+1)P$ transition is the strongest in our experiment conditions (see Sec. 5 for details). Hence this leads to a two stage processes. Rydberg $nD_{5/2}$ state will decay to $(n+1)P_{3/2}$ through spontaneous decay. The dephasing can then be induced in that regime where dipole-dipoles interactions couple nearly degenerate Rydberg pair states [26, 32]. A full model to describe the dephasing is rather complicated. In this section, we will focus on the dephasing effects with a simplified model, which nonetheless captures the main effects.

Considering the three-level scheme in Fig. 1(a), the dephasing rate of Rydberg state γ_3 is around $\gamma_r + \Gamma_{re} \approx \gamma_r$. Rydberg atom has long lifetimes ($1/\Gamma_{re} \sim n^3$) on the order of 100 μs. γ_r represents the dephasing of the atomic coherence (originated from atomic collisions, residue Doppler effect, dipole-dipole interaction between the Rydberg atoms, finite laser linewidth). The dephasing rate of the intermediate state $|e\rangle$ denotes $\gamma_2 = \gamma_e + \Gamma_{eg}$ with spontaneous decay rate Γ_{eg} and interaction induced decay γ_e. In our physical system, γ_e is much smaller than $\Gamma_{eg} \simeq 2\pi \times 5.2$ MHz, thus $\gamma_2 \approx \Gamma_{eg}$. The collective dissipation can emerge in dense atomic gases, typically through two-body dipolar couplings [32]. Here we adopt the effective dephasing $\gamma_3^{\rm eff}$ (i.e., $\gamma_r = \gamma_3^{\rm eff}$), and seek the relation between the transmission and dipolar interaction induced dephasing.

The dynamics of the effective three-level system can be modeled by the quantum master equation for the many-atom density operator ρ:

$$\dot{\rho} = -i[\hat{H}_{\rm eff}, \rho] + D_1(\rho) + D_{\rm eff}(\rho), \tag{1}$$

The effective Hamiltonian in the equation is given by

$$\begin{aligned}\hat{H}_{\rm eff} = \quad & \sum_{j=1}^{N}\Bigg[-\Delta_p \hat{\sigma}_{ee}^{j}(\mathbf{r},t) - (\Delta_p + \Delta_c)\hat{\sigma}_{rr}^{j}(\mathbf{r},t) + \frac{\Omega_p}{2}\hat{\sigma}_{eg}^{j}(\mathbf{r},t) + \frac{\Omega_c}{2}\hat{\sigma}_{re}^{j}(\mathbf{r},t) \\ & + \sum_{k\neq j}^{N}\frac{V_{jk}}{2}\hat{\sigma}_{rr}^{j}\hat{\sigma}_{rr}^{k} + {\rm H.c.}\Bigg],\end{aligned} \tag{2}$$

with $\hat{\sigma}_{ab}(z_j) \equiv |a_j\rangle\langle b_j|$ (z_j is the position of jth atom in the respective ensemble) and H.c. representing Hermitian conjugate of the preceding terms. $V_{jk} = C_6/|\mathbf{r}_j - \mathbf{r}_k|^6$ is the vdW potential with the dispersive coefficient $C_6 \propto n^{11}$. The dissipative effects are described by the Lindblad form $D_1(\rho)$,

$$D_1(\rho) = \sum_{j=1}^{N} \Gamma_{eg} \left(\hat{\sigma}^j_{ge} \rho \hat{\sigma}^j_{eg} - \frac{1}{2}\{\hat{\sigma}^j_{ee}, \rho\} \right), \tag{3}$$

where $D_1(\rho)$ denotes the decay from state $|e\rangle$ to $|g\rangle$. The effective dephasing term $D_{\text{eff}}(\rho)$ is introduced,

$$D_{\text{eff}}(\rho) = \sum_{j=1}^{N} \gamma_3^{\text{eff}} \left(\hat{\sigma}^j_{33} \rho \hat{\sigma}^j_{33} - \frac{1}{2}\{\hat{\sigma}^j_{33}, \rho\} \right), \tag{4}$$

Due to the dephasing and spectral shift of the transparency resonance [see Fig.2(a)], we employ the theoretical description of individual atoms coupled to a mean field (MF) to analyze the EIT spectrum with strong Rydberg interactions [34–36]. In the MF approximation, the many-body density matrix ρ is decoupled into individual ones through $\hat{\rho} \approx \Pi_i \hat{\rho}_i$. In the thermodynamic limit, the optical Bloch equations for the three-level system can be obtained, where elements of the density matrix are represented with $\rho_{ab} = N^{-1} \sum_j \langle \hat{\sigma}^j_{ab} \rangle$. As indicated in our experiment, over a long time evolution, the interactions between Rydberg state leads to a MF shift where $\Delta_c \rightarrow \Delta_c + V\rho_{rr}$ with MF interaction energy $V = N^{-1} \sum_{k \neq j} V_{jk}$.

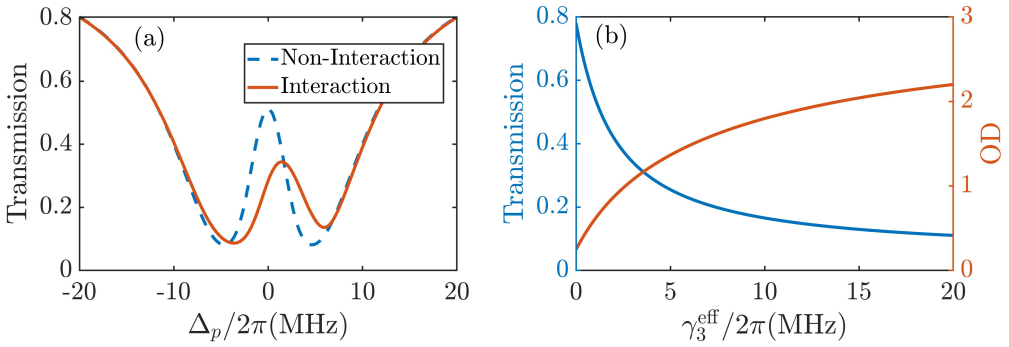

Fig. 4. (a) Theoretical results of EIT transmission varies with Δ_p for $V = 0$ and $V \neq 0$. (b) EIT transmission and corresponding OD versus effective dephasing rate γ_3^{eff} of Rydberg state that accounts for the interaction between Rydberg atoms with $\Omega_p/2\pi$ =1.04 MHz, $\Omega_c/2\pi$ =10.6 MHz and atomic density $1\times10^{11}\text{cm}^{-3}$.

By numerically solving the MF Bloch equation, one can obtain EIT transmission varies with Δ_p. As shown in Fig. 4(a), there is an increasing blue shift of transparency away from the non-interaction EIT resonance. This is because that the shifted Rydberg state detunes the EIT windows. The similar EIT signal is also observed experimentally [see Fig.2(a)]. To obtain the dependence of the EIT transmission on the effective dephasing induced by Rydberg interactions, we calculate EIT spectra for a series of effective γ_3^{eff}, accounting for the many-body dephasing by Rydberg atoms. In Fig. 4(b), the EIT transmission as a function of γ_3^{eff} is plotted. The system works at two-photon detuning $\delta = 0$ with the probe $\Omega_p/2\pi$ =1.04 MHz, $\Omega_c/2\pi$ =10.6 MHz and atomic density $N_a = 1 \times 10^{11}$ cm^{-3}. It shows that the EIT transmission decrease with γ_3^{eff}. The EIT transmission decreases to 50% when $\gamma_3^{\text{eff}} = 2\pi \times 1.5$ MHz. It is consistent with the trend

of our experimental data [see Fig. 2(a)]. For comparing, we also plot the corresponding OD in Fig. 4(b), as expected, calculated OD of the probe beam increase as γ_3^{eff}. We should note that the presented theoretical model is based on MF equation by simply varying the effective decay rate γ_3^{eff}. Beyond the present model, many-body quantum model need to be developed to gain better understanding of the metastable dynamics [27, 28]. We will discuss it somewhere else.

5. Test of the decay in $80D_{5/2}$ state

The dephasing effects arise from many physical reasons, e.g., atomic collisions, residue Doppler effect, depopulation between the Rydberg atoms, or finite laser linewidth. To test the collective dephasing process, we also conduct the experiment to measure the fast population transfer from $80D_{5/2}$ to $81P_{3/2}$. For $80D_{5/2}$ state used in this work, the space to nearest $81P_{3/2}$ state is 1.3124 GHz, corresponding dipole matrix element 5649.1 ea_0 with e electron charge and a_0 Bohr radius. Therefore, $80D_{5/2}$ Rydberg state displays strong dipole interactions with $81P_{3/2}$, resulting to the state transfer of $80D_{5/2} \rightarrow 81P_{3/2}$ [33]. This transformation leads to the decay of $80D_{5/2}$ Rydberg atoms and further decreases of EIT transmission. In order to verify this conjecture, we carry out more test that is performed in an additional MOT [not shown in Fig. 1(b)], in which Rydberg atoms is detected with a state select field ionization detection. The temperature of the atomic cloud is almost same with the main setup, and the peak density of atomic cloud is $8.0 \times 10^{10} cm^{-3}$, which is comparable with the main setup of $1.0 \times 10^{11} cm^{-3}$. In addition, we make the probe and coupling Rabi frequency on the almost same to that of the main setup so that the Rydberg population is comparable with that of the EIT in the main apparatus. Therefore, we obtain the similar EIT spectra and field ionization signal simultaneously in the test setup. The details of the setup can be seen in our previous work [33, 37]. In the test experiments, after switching off the MOT beams, we apply a two-photon excitation pulse with duration 4 μs for preparing $80D_{5/2}$ Rydberg atoms, an optional interaction time t_{INT} before the ionization detection allows us to study the decay of $80D_{5/2}$ Rydberg and state transformation.

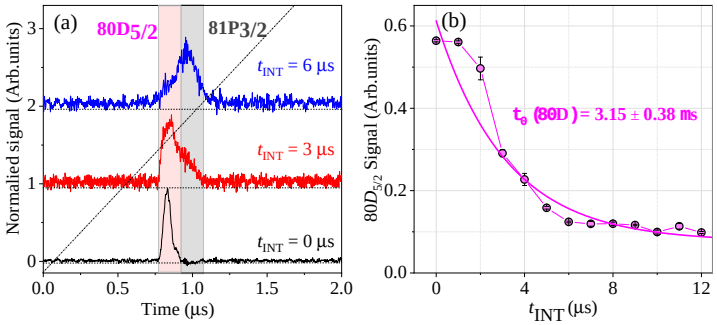

Fig. 5. (a) Normalized time of flight (TOF) signals for laser excitation to $80D_{5/2}$ state with indicated interaction times, t_{INT}. The three traces are set vertically offset for clarity, with the respective zero levels shown as horizontal dashed lines. The gates for the $80D_{5/2}$ and $81P_{3/2}$ states signals are shown as a light pink and gray shaded regions, respectively. (b) Measurements of the $80D_{5/2}$ state as a function of the interaction time t_{INT}. Initial prepared $80D_{5/2}$ Rydberg atoms transfer to nearby Rydberg states $|r'\rangle$ during t_{INT} due to the strong resonant dipole interaction. The solid line shows the exponential fitting with the characteristic time $\tau_{0(80D)}$ = 3.15 ± 0.38 μs.

In Fig. 5(a), we present the time of flight (TOF) signals for laser excitation to $80D_{5/2}$ state. Initially, atoms are populated in $80D_{5/2}$ state (see the black curve) in the TOF signal. Due to the

resonant dipole interaction, atoms in $80D_{5/2}$ state in light pink shaded region partly transfer to nearby $81P_{3/2}$ state in the gray shaded region [see the red curve for $t_{\rm INT}$ = 3 μs]. With further increasing $t_{\rm INT}$, most of $80D_{5/2}$ state Rydberg atoms transfer to $81P_{3/2}$ state (see the blue curve for $t_{\rm INT}$ = 6 μs). The population in state $81P_{3/2}$ reaches maximal at $t_{\rm INT}$ = 6 μs, and then decays to other states. For better understanding of the transfer process, we make a series of measurements for different $t_{\rm INT}$. Figure 5(b) displays the measured $80D_{5/2}$ as a function of $t_{\rm INT}$. It is clear to observe the fast decay process on $80D_{5/2}$ state within 8μs. To obtain the decay characteristic of $80D_{5/2}$ state, we fit the experimental data using exponential function [see the solid line of Fig. 5(b)]. The fitted results show decay time $\tau_{0(80D)}$ = 3.15 ± 0.38 μs is close to the decay of the EIT transmission rate $\tau_{0(EIT)}$. Therefore, we conclude that the dipole interaction induced the state transfer may be the reason that leads to the decay of $80D_{5/2}$ Rydberg three-level EIT transmission.

6. Conclusion

We have presented Rydberg EIT spectra in a cascade three-level scheme involving $80D_{5/2}$ state of Cs atoms. Rydberg EIT spectrum shows strong dependence on the probe incident photon number. The optical transmission displays decay behavior with time. An optical depth of the medium is defined to characterize the transmission. We have shown that the optical depth displays linear increase with the time at onset for fixed probe $R_{\rm in}$. We have further obtained the dephasing rate $\gamma_{\rm OD}$ by redefining OD=$\gamma_{\rm OD}t$. The dephasing rate linearly increases with weak probe field and then saturates for large $R_{\rm in}$. We have shown that the dephasing mechanism is mainly attributed to the strong dipole-dipole interactions, which lead to strong population decay on $|nD_{5/2}\rangle$ state. The experimental setting provides a platform to explore quantum nonlinear optics and quantum information processing, and creates metastable state in quantum many-body systems.

Funding. The work was supported by the National Nature Science Foundation of China (Grant Nos. 61835007, 12120101004, 62175136, 12104337, 11904104, 12274131, 12241408), the Changjiang Scholars and Innovative Research Team in University of Ministry of Education of China (Grant No. RTIRT 17R70), 1331 project of Shanxi province, the scientific cooperation exchanges project of Shanxi province (Grant No. 202104041101015), the Shanghai Pujiang Program (Grant No. 21PJ1402500), the EPSRC (Grant No. EP/W015641/1).

Disclosures. The authors declare no conflicts of interest.

Data Availability Statement. Data underlying the results presented in this paper are not publicly available at this time but may be obtained from the authors upon reasonable request.

References

1. T. F. Gallagher, *Rydberg Atoms* (Cambridge University Press, Cambridge, 1994).
2. D. Jaksch, J. I. Cirac, P. Zoller, S. L. Rolston, R. Côté, and M. D. Lukin, "Fast quantum gates for neutral atoms," Phys. Rev. Lett. **85**, 2208–2211 (2000).
3. D. Viscor, W. Li, and I. Lesanovsky, "Electromagnetically induced transparency of a single-photon in dipole-coupled one-dimensional atomic clouds," New J. Phys. **17** (2015).
4. L. Isenhower, E. Urban, X. L. Zhang, A. T. Gill, T. Henage, T. A. Johnson, T. G. Walker, and M. Saffman, "Demonstration of a Neutral Atom Controlled-NOT Quantum Gate," Phys. Rev. Lett. **104**, 010503 (2010).
5. I. M. Georgescu, S. Ashhab, and F. Nori, "Quantum simulation," Rev. Mod. Phys. **86** (2014).
6. J. D. Pritchard, D. Maxwell, A. Gauguet, K. J. Weatherill, M. P. Jones, and C. S. Adams, "Cooperative atom-light interaction in a blockaded Rydberg ensemble," Phys. Rev. Lett. **105** (2010).
7. V. Parigi, E. Bimbard, J. Stanojevic, A. J. Hilliard, F. Nogrette, R. Tualle-Brouri, A. Ourjoumtsev, and P. Grangier, "Observation and Measurement of Interaction-Induced Dispersive Optical Nonlinearities in an Ensemble of Cold Rydberg Atoms," Phys. Rev. Lett. **109**, 233602 (2012).
8. T. Peyronel, O. Firstenberg, Q. Y. Liang, S. Hofferberth, A. V. Gorshkov, T. Pohl, M. D. Lukin, and V. Vuletić, "Quantum nonlinear optics with single photons enabled by strongly interacting atoms," Nature **488**, 57–60 (2012).
9. K. Singer, J. Stanojevic, M. Weidemüller, and R. Côté, "Long-range interactions between alkali Rydberg atom pairs correlated to the n s– n s, n p– n p and n d– n d asymptotes," J. Phys. B At. Mol. Opt. Phys. **38**, S295–S307 (2005).

10. B. Vermersch, A. W. Glaetzle, and P. Zoller, "Magic distances in the blockade mechanism of rydberg p and d states," Phys. Rev. A **91**, 023411 (2015).
11. Y.-C. Jiao, X.-X. Han, Z.-W. Yang, J.-M. Zhao, and S.-T. Jia, "Electromagnetically Induced Transparency in a Cold Gas with Strong Atomic Interactions," Chin. Phys. Lett. **33**, 123201 (2016).
12. T. Vogt, M. Viteau, J. Zhao, A. Chotia, D. Comparat, and P. Pillet, "Dipole blockade at förster resonances in high resolution laser excitation of rydberg states of cesium atoms," Phys. Rev. Lett. **97**, 6–9 (2006).
13. D. Comparat and P. Pillet, "Dipole blockade in a cold rydberg atomic sample," J. Opt. Soc. Am. B **27**, A208–A232 (2010).
14. S. Sevinçli, N. Henkel, C. Ates, and T. Pohl, "Nonlocal nonlinear optics in cold rydberg gases," Phys. Rev. Lett. **107**, 153001 (2011).
15. Z. Bai and G. Huang, "Enhanced third-order and fifth-order Kerr nonlinearities in a cold atomic system via Rydberg-Rydberg interaction," Opt. Express **24**, 4442–4461 (2016).
16. C. Chen, F. Yang, X. Wu, C. Shen, M. K. Tey, and L. You, "Two-color optical nonlinearity in an ultracold rydberg atom gas mixture," Phys. Rev. A **103**, 053303 (2021).
17. J. A. Sedlacek, A. Schwettmann, H. Kübler, R. Löw, T. Pfau, and J. P. Shaffer, "Microwave electrometry with rydberg atoms in a vapour cell using bright atomic resonances," Nat. physics **8**, 819–824 (2012).
18. Y. O. Dudin and A. Kuzmich, "Strongly Interacting Rydberg Excitations of a Cold Atomic Gas," Science **336**, 887–889 (2012).
19. S. Baur, D. Tiarks, G. Rempe, and S. Dürr, "Single-Photon Switch Based on Rydberg Blockade," Phys. Rev. Lett. **112**, 1–5 (2014).
20. L. Li, Y. O. Dudin, and A. Kuzmich, "Entanglement between light and an optical atomic excitation," Nature **498**, 466–469 (2013).
21. D. Tiarks, S. Baur, K. Schneider, S. Dürr, and G. Rempe, "Single-photon transistor using a Förster resonance," Phys. Rev. Lett. **113** (2014).
22. Y. Ding, Z. Bai, G. Huang, and W. Li, "Facilitation Induced Transparency and Single Photon Switch with Dual-Channel Rydberg Interactions," arXiv:2205.14621 (2022).
23. H. Gorniaczyk, C. Tresp, J. Schmidt, H. Fedder, and S. Hofferberth, "Single-photon transistor mediated by interstate Rydberg interactions," Phys. Rev. Lett. **113**, 1–5 (2014).
24. H. Gorniaczyk, C. Tresp, P. Bienias, A. Paris-Mandoki, W. Li, I. Mirgorodskiy, H. P. Büchler, I. Lesanovsky, and S. Hofferberth, "Enhancement of Rydberg-mediated single-photon nonlinearities by electrically tuned Förster resonances," Nat. Commun. **7**, 12480 (2016).
25. S. Ravets, H. Labuhn, D. Barredo, T. Lahaye, and A. Browaeys, "Measurement of the angular dependence of the dipole-dipole interaction between two individual Rydberg atoms at a Förster resonance," Phys. Rev. A **92**, 020701 (2015).
26. C. Tresp, P. Bienias, S. Weber, H. Gorniaczyk, I. Mirgorodskiy, H. P. Büchler, and S. Hofferberth, "Dipolar Dephasing of Rydberg D-State Polaritons," Phys. Rev. Lett. **115**, 083602 (2015).
27. K. Macieszczak, M. u. u. u. u. Guţă, I. Lesanovsky, and J. P. Garrahan, "Towards a theory of metastability in open quantum dynamics," Phys. Rev. Lett. **116**, 240404 (2016).
28. K. Macieszczak, Y. Zhou, S. Hofferberth, J. P. Garrahan, W. Li, and I. Lesanovsky, "Metastable decoherence-free subspaces and electromagnetically induced transparency in interacting many-body systems," Phys. Rev. A **96**, 043860 (2017).
29. Y. Jiao, J. Li, L. Wang, H. Zhang, L. Zhang, J. Zhao, and S. Jia, "Laser frequency locking based on Rydberg electromagnetically induced transparency," Chin. Phys. B **25**, 053201 (2016).
30. M. Fleischhauer, A. Imamoglu, and J. P. Marangos, "Electromagnetically induced transparency: Optics in coherent media," Rev. Mod. Phys. **77**, 633–673 (2005).
31. L. Hao, Y. Jiao, Y. Xue, X. Han, S. Bai, J. Zhao, and G. Raithel, "Transition from electromagnetically induced transparency to Autler–Townes splitting in cold cesium atoms," New J. Phys. **20**, 073024 (2018).
32. D. Yan, B. Wang, Z. Bai, and W. Li, "Electromagnetically induced transparency of interacting rydberg atoms with two-body dephasing," Opt. Express **28**, 9677–9689 (2020).
33. L. Hao, Z. Bai, J. Bai, S. Bai, Y. Jiao, G. Huang, J. Zhao, W. Li, and S. Jia, "Observation of blackbody radiation enhanced superradiance in ultracold rydberg gases," New J. Phys. **23**, 083017 (2021).
34. H. Schempp, G. Günter, C. S. Hofmann, C. Giese, S. D. Saliba, B. D. DePaola, T. Amthor, M. Weidemüller, S. Sevinçli, and T. Pohl, "Coherent population trapping with controlled interparticle interactions," Phys. Rev. Lett. **104**, 173602 (2010).
35. J. D. Pritchard, D. Maxwell, A. Gauguet, K. J. Weatherill, M. P. A. Jones, and C. S. Adams, "Cooperative atom-light interaction in a blockaded rydberg ensemble," Phys. Rev. Lett. **105**, 193603 (2010).
36. J. Han, T. Vogt, and W. Li, "Spectral shift and dephasing of electromagnetically induced transparency in an interacting rydberg gas," Phys. Rev. A **94**, 043806 (2016).
37. X. Han, S. Bai, Y. Jiao, L. Hao, Y. Xue, J. Zhao, S. Jia, and G. Raithel, "Cs 62DJ Rydberg-atom macrodimers formed by long-range multipole interaction," Phys. Rev. A **97** (2018).